

RESEARCH

Open Access



Systemic immune-related spleen radiomics predict progression-free survival in patients with locally advanced cervical cancer underwent definitive chemoradiotherapy

Yi Li^{1†}, Longxiang Guo^{1†}, Peng Xie², Yuhui Liu³, Yuanlin Li⁴, Ao Liu^{5,6*} and Minghuan Li^{1*}

Abstract

Purpose Systemic immunity is essential for driving therapeutically induced antitumor immune responses, and the spleen may reflect alterations in systemic immunity. This study aimed to evaluate the predictive value of contrast-enhanced CT-based spleen radiomics for progression-free survival (PFS) in patients with locally advanced cervical cancer (LACC) who underwent definitive chemoradiotherapy (dCRT). Additionally, we investigated the role of spleen radiomics features and changes in spleen volume in assessing systemic immunity.

Methods This retrospective study included 257 patients with LACC who underwent dCRT. The patients were randomly divided into training and validation groups in a 7:3 ratio. Radiomic features were extracted from CT images obtained before and after dCRT. Radiomic scores (Radscore) were calculated using features selected through least absolute shrinkage and selection operator (LASSO) Cox regression. The percentage change in spleen volume was determined from measurements taken before and after treatment. Independent prognostic factors for PFS were identified through multivariate Cox regression analyses. Model performance was evaluated with the receiver operating characteristic (ROC) curve and the C-index. The Radscore cut-off value, determined from the ROC curve, was used to stratify patients into high- and low-risk survival groups. The Wilcoxon test was used to analyze differences in hematological parameters between different survival risk groups and between different spleen volume change groups. Spearman correlation analysis was used to explore the relationship between spleen volume change and hematological parameters.

Results Independent prognostic factors included FIGO stage, pre-treatment neutrophil-to-lymphocyte ratio (pre-NLR), spleen volume change, and Radscore. The radiomics-combined model demonstrated the best predictive performance for PFS in both the training group (AUC: 0.923, C-index: 0.884) and the validation group (AUC: 0.895, C-index: 0.834). Compared to the low-risk group, the high-risk group had higher pre-NLR ($p=0.0054$) and post-NLR

[†]Yi Li and Longxiang Guo contributed equally to this work.

*Correspondence:

Ao Liu

liuao@sdu.edu.cn

Minghuan Li

sdlmh2014@163.com

Full list of author information is available at the end of the article



© The Author(s) 2024. **Open Access** This article is licensed under a Creative Commons Attribution-NonCommercial-NoDerivatives 4.0 International License, which permits any non-commercial use, sharing, distribution and reproduction in any medium or format, as long as you give appropriate credit to the original author(s) and the source, provide a link to the Creative Commons licence, and indicate if you modified the licensed material. You do not have permission under this licence to share adapted material derived from this article or parts of it. The images or other third party material in this article are included in the article's Creative Commons licence, unless indicated otherwise in a credit line to the material. If material is not included in the article's Creative Commons licence and your intended use is not permitted by statutory regulation or exceeds the permitted use, you will need to obtain permission directly from the copyright holder. To view a copy of this licence, visit <http://creativecommons.org/licenses/by-nc-nd/4.0/>.

($p=0.038$). Additionally, compared to the decreased spleen volume group, the increased spleen volume group had lower post-NLR ($p=0.0059$) and post-treatment platelet-to-lymphocyte ratio ($p<0.001$).

Conclusion Spleen radiomics combined with clinical features can effectively predict PFS in patients with LACC after dCRT. Furthermore, spleen radiomics features and changes in spleen volume can reflect alterations in systemic immunity.

Keywords Cervical cancer, Radiomics, Spleen, Computed tomography, Systemic immunity

Introduction

Cervical cancer is the fourth most common cancer and the fourth leading cause of cancer deaths among women globally, posing a significant health threat, particularly in developing countries [1–3]. Currently, the primary treatment for locally advanced cervical cancer (LACC) is definitive chemoradiotherapy (dCRT) [4–7]. The addition of radiotherapy significantly enhances both the local control rate and survival in LACC. This is attributed to the efficacy of radiotherapy, which not only directly kills tumor cells but also modulates systemic immunity, thereby enhancing immune responses and strengthening tumor control [8, 9]. The duration of effective tumor control by radiotherapy correlates with radiation-induced tumor equilibrium, which depends on an adequate quantity and quality of T cells capable of suppressing spontaneous tumor metastasis and maintaining tumor cell dormancy [10–13].

The spleen, a crucial immune organ outside the tumor microenvironment, regulates both innate and adaptive immune responses and plays a significant role in tumor-host interactions and systemic immunity [14]. During tumor development, the spleen, bone marrow, blood, and draining lymph nodes form an interconnected immune network that remains in constant communication. Allen et al. [15] observed a positive correlation between the total cell count of tumor-infiltrating leukocytes and tumor size, along with an increase in splenic cell count during tumor growth. Furthermore, the immune cell status of each immune organ changes dynamically throughout this process. Notably, the characteristics of the spleen and blood are remarkably similar, particularly with the reorganization of T cell subpopulations dominated by CD4+T cells. Additionally, spleen metabolic activity correlates with systemic inflammatory markers and can predict prognosis in patients with rectal, gastric, breast, and cervical cancers [16–19]. These findings collectively suggest a close interconnection between the spleen, tumors, and systemic immunity. Thus, the spleen could serve as a monitoring station for changes in immune-related hematological parameters, potentially aiding in the prediction of tumor progression.

Radiomics is a promising predictive approach that reflects tumor heterogeneity by analyzing standard medical image features, offering high-throughput quantitative

information. It has demonstrated significant predictive performance for treatment response and clinical outcomes [20, 21]. Spleen radiomics is increasingly gaining attention for its ability to predict recurrence and prognosis in patients [22, 23]. This study aimed to evaluate the predictive value of spleen radiomics for progression-free survival (PFS) in patients with LACC following dCRT. Additionally, we explored the correlation between spleen radiomics and systemic immune-related hematological parameters, such as absolute lymphocyte count (ALC), neutrophil-to-lymphocyte ratio (NLR), and platelet-to-lymphocyte ratio (PLR), to elucidate the underlying mechanisms [24, 25]. We also examined changes in spleen volume after dCRT and its correlation with PFS, and investigated the differences in hematological parameters associated with varying changes in spleen volume.

Materials and methods

Patients

This retrospective study included 257 patients with LACC who were treated with dCRT between December 2017 and July 2021. The inclusion criteria were as follows: (1) newly diagnosed and pathologically confirmed LACC; (2) completion of a standard radiotherapy program; (3) age ≤ 75 years; (4) no history of previous splenic surgery; and (5) availability of complete CT images and hematology data within 1 month before and 3 months after treatment, as well as comprehensive clinical and pathological data. The exclusion criteria were as follows: (1) presence of other tumors; (2) patients with cirrhosis and splenomegaly; (3) presence of acute infection or autoimmune disease; (4) long-term use of glucocorticoid drugs; and (5) loss of visit or failure to review as required. All patients who met the criteria were randomly divided into a training group and a validation group at a 7:3 ratio (Fig. 1).

Treatment and follow-up

The treatment protocol adhered to both domestic and international guidelines and norms [26, 27]. Radiotherapy comprised both whole-pelvic external beam radiation therapy (EBRT) and brachytherapy. EBRT was administered to the pelvis using intensity-modulated radiation therapy (IMRT), with a total dose of 45–50.4 Gy delivered at 1.8–2.0 Gy per fraction in 25–28 fractions. For patients with positive lymph nodes, an additional 10–15 Gy was

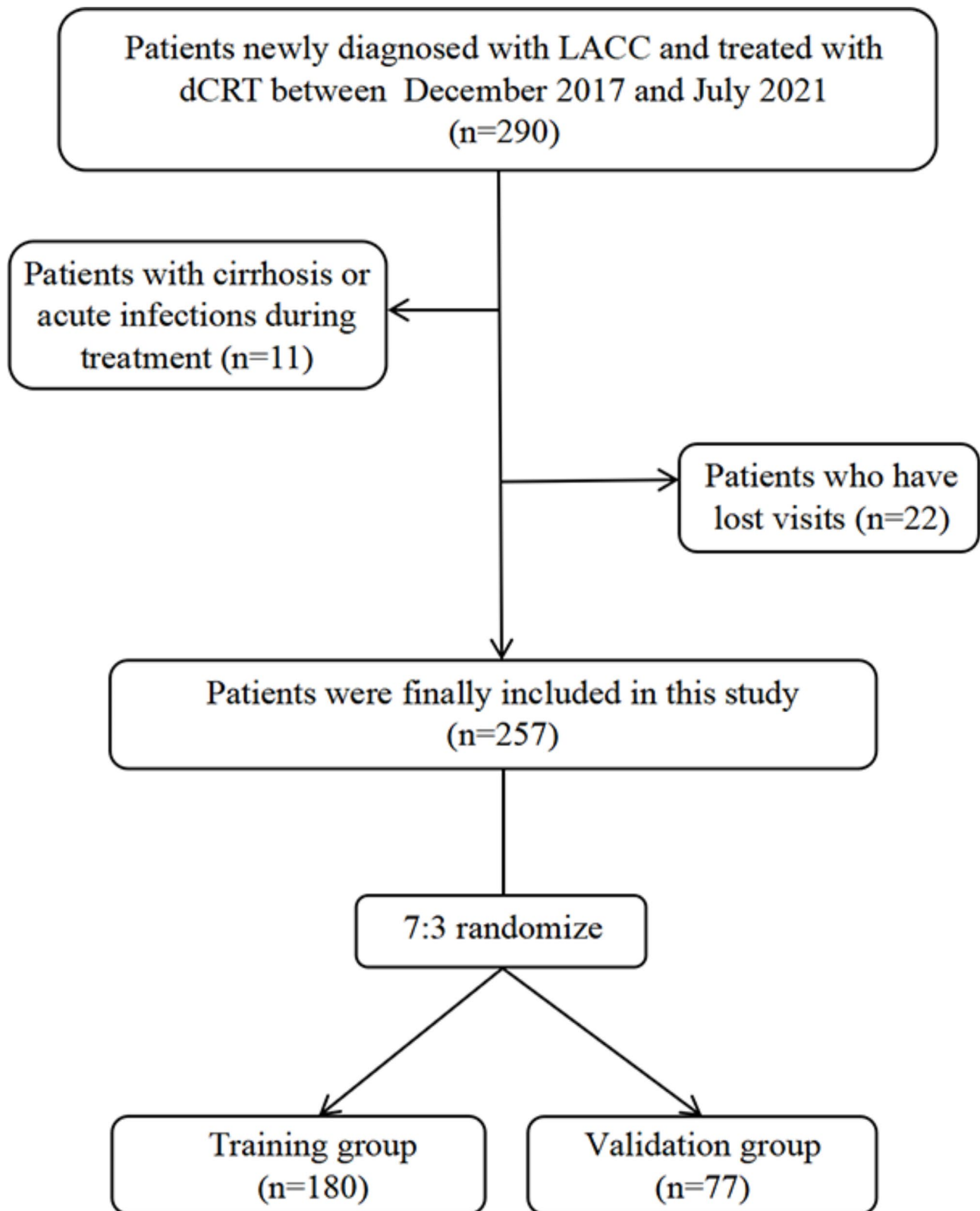


Fig. 1 Recruitment and selection process of patients

delivered using a simultaneous integrated boost (SIB) technique, with the SIB to the gross target (positive lymph nodes) administered at up to 2.2 Gy per fraction. Brachytherapy predominantly employed a point-A based technique, delivering a total dose of 30 to 40 Gy in 6–8 fractions. The cumulative dose of EBRT and brachytherapy reached 80–90 Gy. Patients received 3–6 cycles of concurrent chemotherapy during radiotherapy, primarily consisting of weekly cisplatin (40 mg/m²). Follow-up was conducted approximately every 3 months for the first 2 years after the completion of therapy, every 6 months for the subsequent 3 to 5 years, and annually thereafter. The follow-up primarily consisted of regular outpatient and inpatient evaluations, along with telephone communication. The evaluation primarily included gynecological examinations, hematological analysis, and enhanced CT scans of the pelvis, chest, and abdomen. Three months post-treatment, efficacy was assessed using imaging and gynecological examinations according to the Response Evaluation Criteria in Solid Tumors (RECIST) [28]. PFS was measured in months and defined as the period from treatment commencement to either the initial diagnosis of disease progression, death, or until the latest follow-up.

Image acquisition and segmentation

All patients underwent standard pelvic and abdominal enhanced CT within 1 month before and 3 months after treatment. A 64-layer spiral CT scanner (Definition AS+; Siemens SOMATOM) was used for CT image acquisition. The scanning parameters were as follows: a slice thickness of 5.0 mm, tube voltage of 120 kV, and tube current of 220 mA. We exported the DICOM format files corresponding to the enhanced CT images of all patients through the PCAS (Picture Archiving and

Communication System) and imported them as raw images into 3D Slicer software (version 5.4.0, USA). The spleen was manually delineated as the region of interest (ROI) by a radiation oncologist under the guidance of an experienced radiologist, with deliberate avoidance of large splenic vessels during the outlining process. The final segmentation was then personally examined by the experienced radiologist. A flowchart of the main steps is shown in Fig. 2.

Selection of radiomics features and radscore construction

We used PyRadiomics, an open-source package within the 3D Slicer software, to extract features from the pre- and post-treatment CT images of each patient, respectively. These features included seven types: shape, first-order, gray level co-occurrence matrix (GLCM), gray level run length matrix (GLRLM), gray level size zone matrix (GLSZM), gray level dependence matrix (GLDM), and neighborhood gray-tone difference matrix (NGTDM). Delta-radiomics features were obtained by subtracting the pre-treatment radiomics features from the post-treatment radiomics features. Subsequently, 30 patients were randomly selected from the training group, and their spleens were re-outlined by another experienced radiologist for intra-group correlation coefficient (ICC) analysis. Only stable features with ICC values ≥0.8 were retained. To ensure comparability between data of varying magnitudes, Z-score standardization was applied to normalize the data. Using R software (version 4.3.2), we employed least absolute shrinkage and selection operator (LASSO) Cox regression analysis with 10-fold cross-validation to select features associated with PFS. The radiomics score (Radscore) for each patient was calculated as a linear combination of the selected

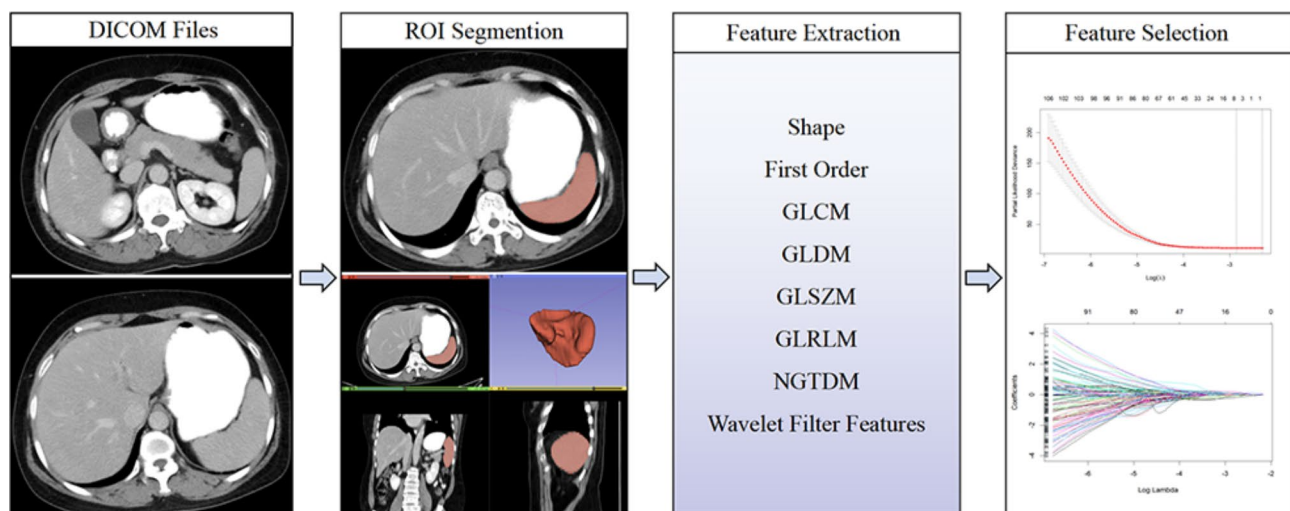


Fig. 2 Workflow of the study

features, with weights assigned based on their respective coefficients.

Calculation of spleen volume change

Using 3D Slicer software, we analyzed the spleen volumes of patients before and after treatment and calculated the percentage change in spleen volume. The formula is as follows:

$$\begin{aligned} & \text{Spleen Volume Change (\%)} \\ &= \frac{\text{Post-treatment Spleen Volume} - \text{Pre-treatment Spleen Volume}}{\text{Pre-treatment Spleen Volume}} \\ & \times 100\%. \end{aligned}$$

Construction and validation of survival prediction models

Independent prognostic factors for PFS were identified through univariate and multivariate Cox regression analyses. Subsequently, we constructed three models: clinical, radiomics, and radiomics-combined. The optimal performing model was selected to construct a nomogram to achieve a more intuitive prediction. Consequently, we used the receiver operating characteristic (ROC) curve to determine the optimal cut-off value for Radscore. Survival curves for different Radscore were evaluated using the Kaplan–Meier (KM) method, and patients were stratified into high- and low-risk groups. The between-group comparisons were performed using the log-rank test ($p < 0.05$). The models' performance was evaluated using the concordance index (C-index) of the ROC curves. Calibration curves were employed to evaluate the agreement between nomogram predictions and observed patient outcomes.

Correlation analysis between spleen and hematological parameters

The Wilcoxon rank-sum test was used to analyze the differences in immune-related hematological parameters between the two groups of patients classified as high- and low-risk according to the Radscore. Furthermore, patients were stratified into groups based on increased or decreased spleen volume, and then we evaluated the survival curves of the two groups employing the KM method and compared them using the log-rank test ($p < 0.05$). Differences in hematological parameters associated with varying changes in spleen volume were analyzed using the Wilcoxon rank-sum test. Correlations between changes in spleen volume and hematological parameters were assessed using Spearman correlation analysis.

Finally, we identified independent risk factors for distant metastasis through univariate and multivariate logistic regression analyses, considering factors such as spleen radiomics, spleen volume change, immune-related hematological parameters, and other clinical characteristics.

Statistical analysis

The radiotherapy dose was dichotomized using the median value as the cut-off. Other continuous variables were dichotomized based on the optimal cut-off values determined from ROC curves. Differences between the training and validation groups were evaluated using the t-test (continuous variables) and chi-square test (categorical variables). Statistical analysis was performed using SPSS 27.0.1 and R software 4.3.2. P-values below 0.05 were considered to indicate statistical significance when interpreting the results.

Results

Patient characteristics

A total of 257 patients were included in this study and randomly divided into training ($n=180$) and validation ($n=77$) groups at a ratio of 7:3. There were no statistically significant differences in clinical data between the two groups (Table 1). The median follow-up time was 50.2 months (interquartile range [IQR]: 29.9 to 54.1). Tumor progression occurred in 51 (19.8%) patients during the follow-up period. The highest incidence was of distant metastasis alone (54.9%, $n=28$), followed by locoregional recurrences alone (31.4%, $n=16$), and synchronous distant and locoregional recurrences (13.7%, $n=7$). The objective response rate at 3 months post-treatment was 92.2%, with 169 patients achieving a complete response (65.8%) and 68 patients achieving a partial response (26.4%).

Radiomics feature selection

After delineating the ROI using 3D Slicer software, we extracted 1,037 radiomics features from pre- and post-radiotherapy CT images. Only stable features with ICC values ≥ 0.8 were retained after assessing consistency and then normalized using Z-scores. A total of 878 pre-treatment radiomics features, 911 post-treatment radiomics features, and 795 delta-radiomics features were selected for further analysis. Features were finally selected using LASSO Cox regression (Fig. 3). Among these, 7, 5, and 8 non-zero features were retained for pre-treatment radiomics, post-treatment radiomics, and delta-radiomics, respectively. The corresponding coefficients were determined (Table 2). The values of all radiomic features were then multiplied by their coefficients to obtain the Radscore.

Construction and validation of a nomogram

Univariate analysis was performed on the training group, and variables with $p < 0.05$ were included in the multivariate analysis. FIGO stage, pre-treatment NLR (pre-NLR), spleen volume change, and Radscore were identified as statistically significant factors after multivariate analysis (Table 3). Based on these results, three models were

Table 1 Comparison of patients' characteristics between training and validation groups

Variable	Cut-off	Total (n = 257)	Training (n = 180)	Validation (n = 77)	P
Age, n (%)	< 61 years	214 (83.3)	152 (84.4)	62 (80.5)	0.440
	≥ 61 years	43 (16.7)	28 (15.6)	15 (19.5)	
FIGO stage, n (%)	≤ II	66 (25.7)	44 (24.4)	22 (28.6)	0.488
	> II	191 (74.3)	136 (75.6)	55 (71.4)	
Tumor size, cm; mean ± SD	Continuous	4.81 ± 1.47	4.76 ± 1.41	4.91 ± 1.60	0.461
Pelvic LN status, n (%)	N0	178 (69.3)	124 (68.9)	54 (70.1)	0.843
	N1	79 (30.7)	56 (31.1)	23 (29.9)	
Spleen volume change, n (%)	decrease	87 (33.9)	57 (31.7)	30 (39.0)	0.258
	Increase	170 (66.1)	123 (68.3)	47 (61.0)	
BT dose, n (%)	< 30 Gy	22 (8.6)	14 (7.8)	8 (10.4)	0.493
	≥ 30 Gy	235 (91.4)	166 (92.2)	69 (89.6)	
EBRT dose, n (%)	< 50.4 Gy	89 (34.6)	65 (36.1)	24 (31.2)	0.446
	≥ 50.4 Gy	168 (65.4)	115 (63.9)	53 (68.8)	
pre-ALC, n (%)	< 1.1 × 10 ⁹ cells/L	39 (15.2)	28 (15.6)	11 (14.3)	0.795
	≥ 1.1 × 10 ⁹ cells/L	218 (84.8)	152 (84.4)	66 (85.7)	
post-ALC, n (%)	< 0.7 × 10 ⁹ cells/L	223 (86.8)	160 (88.9)	63 (81.8)	0.125
	≥ 0.7 × 10 ⁹ cells/L	34 (13.2)	20 (11.1)	14 (18.2)	
delta-ALC, n (%)	< -0.86 × 10 ⁹ cells/L	191 (74.3)	136 (75.6)	55 (71.4)	0.488
	≥ -0.86 × 10 ⁹ cells/L	66 (25.7)	44 (24.4)	22 (28.6)	
pre-NLR, n (%)	< 3.49	186 (72.4)	134 (74.4)	52 (67.5)	0.256
	≥ 3.49	71 (27.6)	46 (25.6)	25 (32.5)	
post-NLR, n (%)	< 8.09	208 (80.9)	142 (78.9)	66 (85.7)	0.202
	≥ 8.09	49 (19.1)	38 (21.1)	11 (14.3)	
delta-NLR, n (%)	< 15.59	253 (98.4)	177 (98.3)	76 (98.7)	1.000
	≥ 15.59	4 (1.6)	3 (1.7)	1 (1.3)	
pre-PLR, n (%)	< 226.49	182 (70.8)	129 (71.7)	53 (68.8)	0.647
	≥ 226.49	75 (29.2)	51 (28.3)	24 (31.2)	
post-PLR, n (%)	< 787.5	216 (84.1)	152 (84.4)	64 (83.1)	0.790
	≥ 787.5	41 (15.9)	28 (15.6)	13 (16.9)	
delta-PLR, n (%)	< 384.31	179 (69.7)	129 (71.7)	50 (64.9)	0.282
	≥ 384.31	78 (30.3)	51 (28.3)	27 (35.1)	

Abbreviations: FIGO, Fédération Internationale de Gynécologie et d'Obstétrique; LN, lymph node; BT, brachytherapy; EBRT, external beam radiation therapy; ALC, Absolute lymphocyte counts; NLR, Neutrophil-to-lymphocyte ratio; PLR, Platelet-to-lymphocyte ratio

constructed, including clinical, radiomics, and radiomics-combined models. By comparing the ROC curves of the three models (Fig. 4), it was found that the radiomics-combined model outperformed both the radiomics and clinical models alone in predicting PFS, with AUC values of 0.923 for the training group and 0.895 for the validation group. The C-index values for the two groups were 0.884 (95% CI, 0.843–0.926) and 0.834 (95% CI, 0.735–0.933), respectively (Table 4).

The optimal cut-off value for the Radscore was determined by the ROC curve (19.782). KM analysis indicated that patients with a higher Radscore (high-risk group, Radscore ≥ 19.782) exhibited worse PFS than those with a lower Radscore (low-risk group, Radscore < 19.782) (Fig. 5). Utilizing the radiomics-combined model, we constructed a nomogram for predicting PFS (Fig. 6). By incorporating clinically independent prognostic factors and the Radscore, we were able to predict the 1-, 2-, and

3-year PFS for each patient. The results of the calibration curves for both the training and validation cohorts demonstrated the accuracy of the nomogram model in predicting 1-, 2-, and 3-year PFS (Fig. 7).

Correlation of spleen radiomics with immune-related hematological parameters

By comparing immune-related hematological parameters between the high- and low-risk groups, we found that patients in the high-risk group had higher pre-NLR ($p=0.0054$) and post-NLR ($p=0.038$) compared to those in the low-risk group (Fig. 8).

Spleen volume analyses and its association with PFS

The mean spleen volume before and after pelvic radiotherapy was 193.42 mL and 209.15 mL, respectively, with a median spleen volume change of 7.9% (range: -45.4% to +82.3%). The changes in spleen volume for all patients

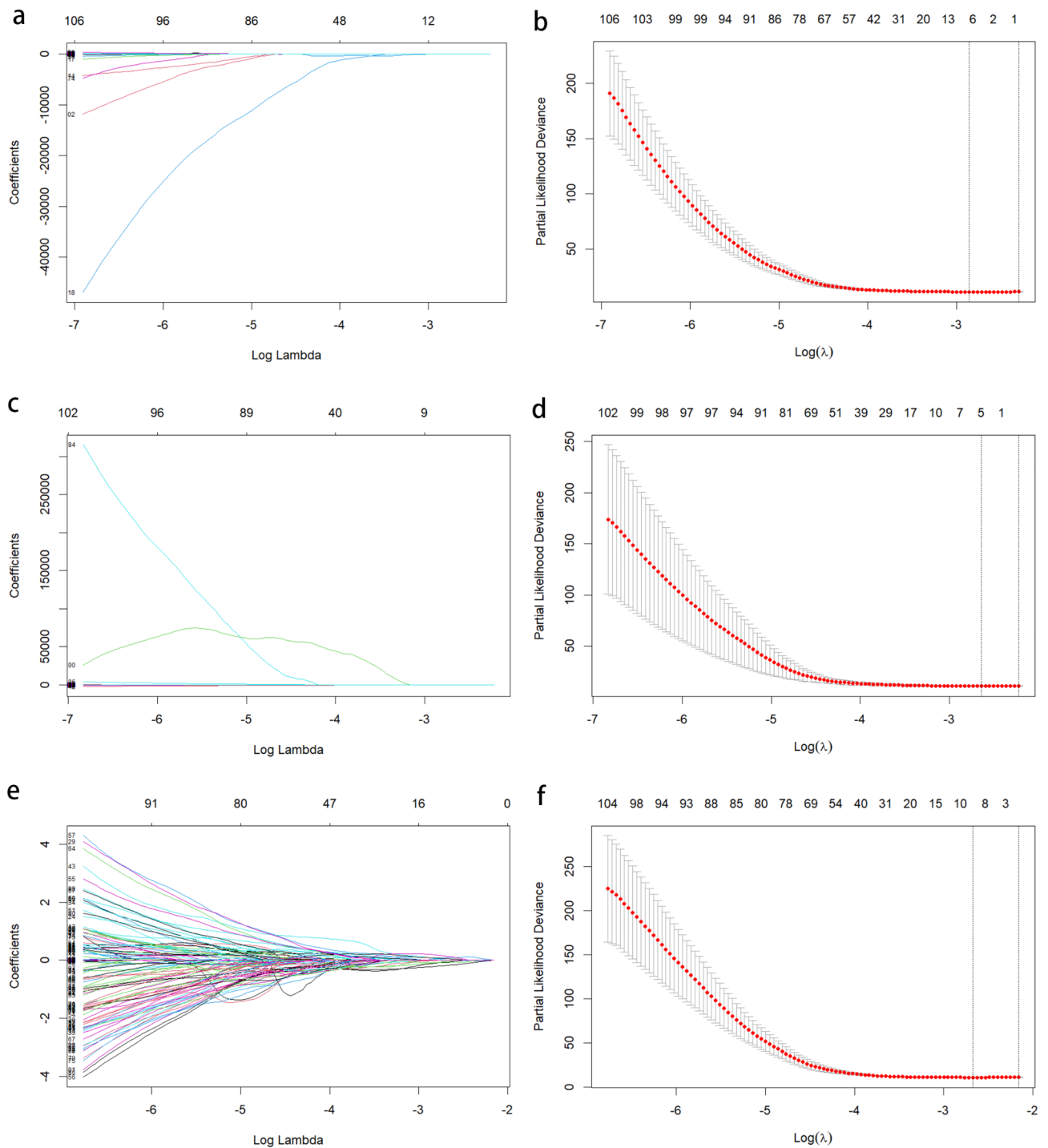


Fig. 3 Selection of radiomic features associated with PFS based on LASSO cox regression models. **a, b** are coefficient and crossvalidation curves of the pre-radiomic features. **c, d** are coefficient and crossvalidation curves of the post-radiomic features. **e, f** are coefficient and crossvalidation curves of the delta-radiomic features

are depicted in the bar plot. (Fig. 9a). We observed an increase in spleen volume in 170 (66.1%) patients and a decrease in spleen volume in 87 (33.9%) patients at 2–3 months after radiotherapy. KM analysis indicated that

patients with increased spleen volume exhibited better PFS than those with decreased spleen volume (log-rank $p < 0.001$) (Fig. 9b and c).

Table 2 Radiomic features associated with PFS selected by LASSO regression

Radiomics features	Coefficients
Pre	
original_shape_Elongation	1.13957147
wavelet.LLH_glszm_LowGrayLevelZoneEmphasis	-0.19664169
wavelet.LHL_ngtdm_Contrast	-0.04497079
wavelet.LHH_glrlm_ShortRunEmphasis	14.91320165
wavelet.HLH_glrlm_ShortRunEmphasis	0.19090070
wavelet.HLH_ngtdm_Strength	-0.02070054
wavelet.HHH_ngtdm_Complexity	2.79738495
Post	
log.sigma.3.0.mm.3D_glrlm_LowGrayLevelRunEmphasis	0.75057599
wavelet.LHL_glcm_lmc1	-0.33751314
wavelet.HLH_firstorder_Mean	-0.15770645
wavelet.HHL_glszm_SizeZoneNonUniformityNormalized	0.08842013
wavelet.HHH_firstorder_Range	0.18775336
Delta	
log.sigma.3.0.mm.3D_gldm_SmallDependenceLowGrayLevelEmphasis	0.09437506
log.sigma.3.0.mm.3D_glrlm_LowGrayLevelRunEmphasis	0.01105204
log.sigma.3.0.mm.3D_glrlm_ShortRunLowGrayLevelEmphasis	0.13354349
log.sigma.5.0.mm.3D_glrlm_RunEntropy	-0.17115025
log.sigma.5.0.mm.3D_glszm_LargeAreaEmphasis	-0.05715490
wavelet.LLH_glszm_LargeAreaEmphasis	-0.07537844
wavelet.HLH_firstorder_Skewness	-0.03417982
wavelet.HLH_ngtdm_Strength	0.05520640

Correlation analysis of spleen volume change and hematological parameters

We compared hematological parameters between patients with increased spleen volume and those with decreased spleen volume. Patients with increased spleen volume had lower NLR ($p=0.0059$) and PLR ($p<0.001$) after radiotherapy compared to those with decreased spleen volume (Fig. 10b and c). Spleen volume change demonstrated a significant negative correlation with NLR ($R = -0.18, p=0.0037$) and PLR ($R = -0.29, p<0.001$) (Fig. 10e and f). Additionally, patients with increased spleen volume had relatively higher ALC, showing a positive correlation after radiotherapy, although this was not statistically significant (Fig. 10a and d). After radiotherapy, the median values of hematological parameters for patients with increased versus decreased spleen volume were as follows: post-ALC, 0.41×10^9 cells/L vs. 0.36×10^9 cells/L; post-NLR, 4.44 vs. 5.61; and post-PLR, 365.09 vs. 513.64.

Predictors of distant metastasis after dCRT

We analyzed the factors associated with distant metastasis. Univariate logistic regression analyses revealed that FIGO stage, tumor size, Radscore, spleen volume change, pre-ALC, delta-ALC, pre-NLR, pre-PLR and post-PLR (all with $p<0.05$) were associated with distant metastasis. Subsequent multivariate analyses demonstrated that Radscore (OR 4.84; 95% CI 1.92–12.24; $p<0.001$) and pre-NLR ≥ 3.49 (OR 2.61; 95% CI 1.04–6.52; $p=0.040$) independently affected distant metastasis (Table 5).

Table 3 PFS-related univariate and multivariate analysis in the training group

Variable	Cut-off	Univariate analysis		Multivariate analysis	
		HR (95%CI)	P	HR (95%CI)	P
Age, years	≥ 61 vs. < 61	1.76 (0.83 ~ 3.73)	0.137		
FIGO stage	$> II$ vs. $\leq II$	6.95 (1.67 ~ 28.88)	0.008	9.96 (2.30 ~ 43.11)	0.002
Tumor size, cm	Continuous	1.19 (0.95 ~ 1.49)	0.134		
Pelvic LN status	N1 vs. N0	1.50 (0.78 ~ 2.91)	0.225		
Spleen volume change	decrease vs. increase	3.97 (2.07 ~ 7.61)	<0.001	2.54 (1.19 ~ 5.44)	0.016
BT dose, Gy	≥ 30 vs. < 30	1.50 (0.36 ~ 6.22)	0.579		
EBRT dose, Gy	≥ 50.4 vs. < 50.4	0.66 (0.35 ~ 1.24)	0.196		
pre-ALC, $\times 10^9$ cells/L	≥ 1.1 vs. < 1.1	0.28 (0.14 ~ 0.55)	<0.001	0.48 (0.13 ~ 1.73)	0.260
post-ALC, $\times 10^9$ cells/L	≥ 0.7 vs. < 0.7	2.36 (1.04 ~ 5.37)	0.040	2.66 (0.87 ~ 8.12)	0.087
delta-ALC, $\times 10^9$ cells/L	≥ -0.86 vs. < -0.86	3.89 (2.06 ~ 7.36)	<0.001	1.65 (0.48 ~ 5.73)	0.430
pre-NLR	≥ 3.49 vs. < 3.49	5.40 (2.83 ~ 10.31)	<0.001	2.91 (1.32 ~ 6.41)	0.008
post-NLR	≥ 8.09 vs. < 8.09	1.35 (0.65 ~ 2.77)	0.421		
delta-NLR	≥ 15.59 vs. < 15.59	2.36 (0.32 ~ 17.23)	0.397		
pre-PLR	≥ 226.49 vs. < 226.49	2.63 (1.39 ~ 4.98)	0.003	0.81 (0.33 ~ 1.94)	0.630
post-PLR	≥ 787.5 vs. < 787.5	1.85 (0.87 ~ 3.90)	0.108		
delta-PLR	≥ 384.31 vs. < 384.31	1.35 (0.69 ~ 2.65)	0.374		
Radscore	Continuous	13.45 (6.52 ~ 27.77)	<0.001	8.46 (4.04 ~ 17.72)	<0.001

Abbreviations: CI, confidence interval; HR: hazard ratio for disease progression or death; FIGO, Fédération Internationale de Gynécologie et d'Obstétrique; LN, lymph node; BT, brachytherapy; EBRT, external beam radiation therapy; ALC, Absolute lymphocyte counts; NLR, Neutrophil-to-lymphocyte ratio; PLR, Platelet-to-lymphocyte ratio

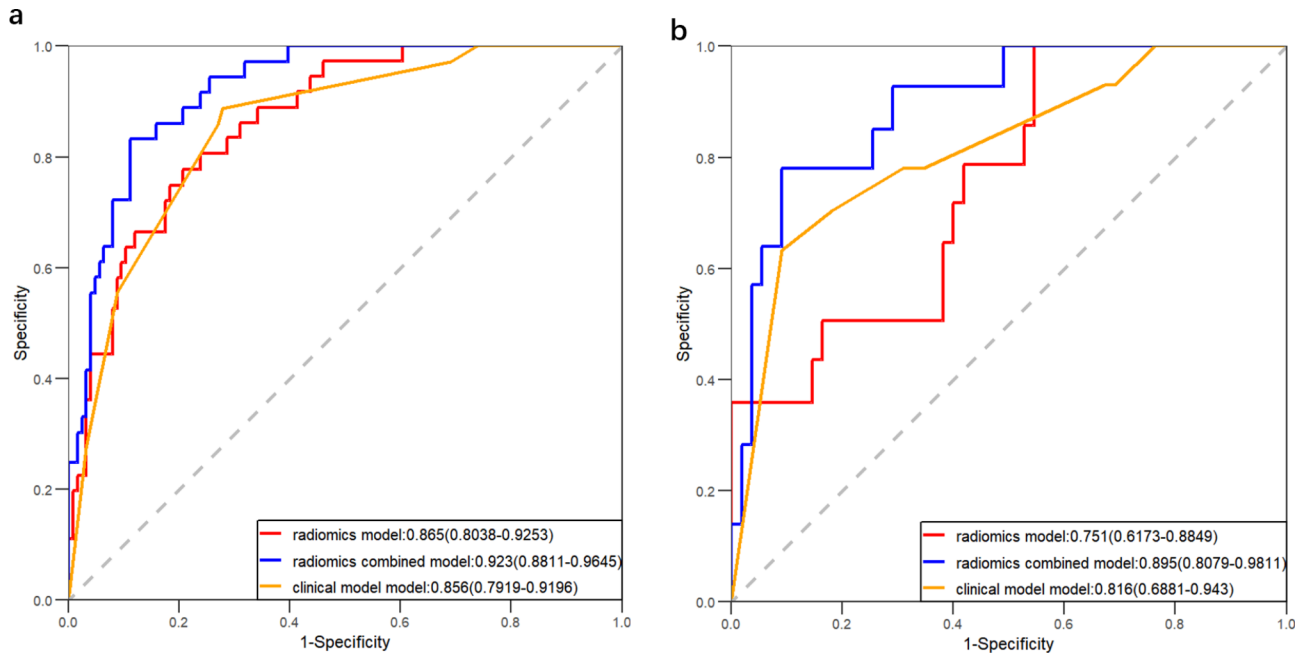


Fig. 4 Receiver Operating Characteristic (ROC) curves constructed based on the three models. **a** and **b** are the ROC curves for predicting PFS in the training and validation groups, respectively

Table 4 The C-index (95% CI) of three models

PFS	Training group (95%CI)	Validation group (95%CI)
clinical model	0.818 (0.761 ~ 0.875)	0.792 (0.692 ~ 0.892)
radiomics model	0.836 (0.781 ~ 0.891)	0.708 (0.588 ~ 0.828)
radiomics-combined model	0.884 (0.843 ~ 0.926)	0.834 (0.735 ~ 0.933)

Discussion

In this study, we developed and evaluated survival prediction models for patients with LACC based on CT images of the spleen. We analyzed three models: clinical,

radiomics, and radiomics-combined. Our findings demonstrated that the radiomics-combined model outperformed both the radiomics and clinical models alone in predicting PFS. It achieved the best performance, with an AUC of 0.895 and a C-index of 0.834 in the validation group. To our knowledge, this is the first study to use spleen radiomics to predict survival in patients with LACC. Recently, the potential of radiomics to predict lymph node metastasis, treatment response, and prognosis in patients with cervical cancer has gained increasing recognition [29–31]. However, these studies were

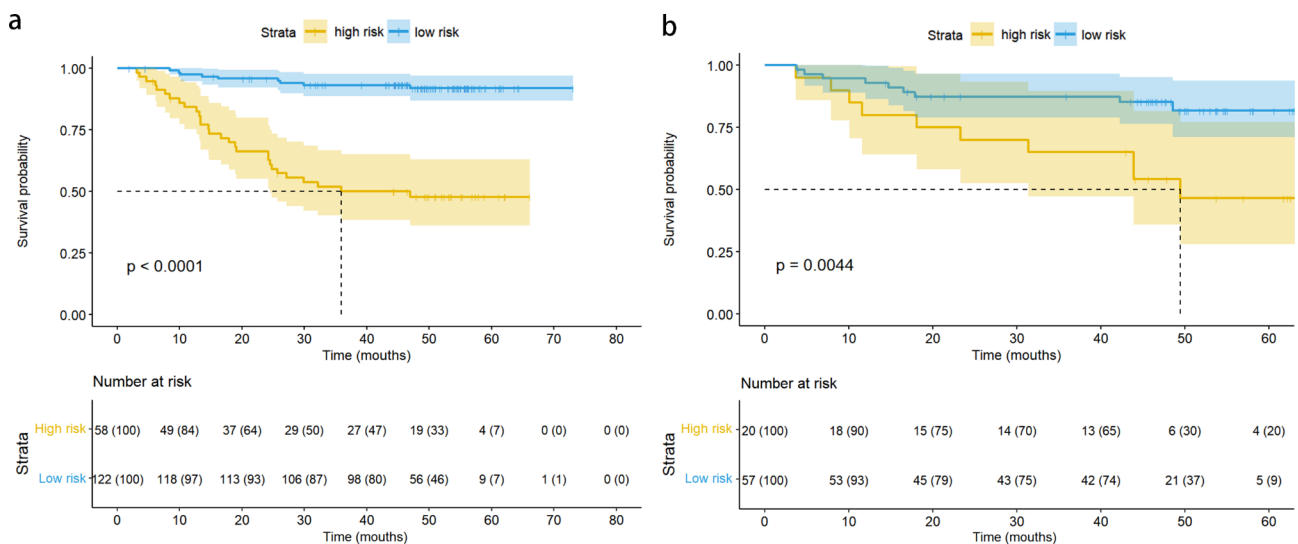


Fig. 5 **a** and **b** are Kaplan-Meier curves for PFS in training group and validation group, with patients stratified according to the RadScore

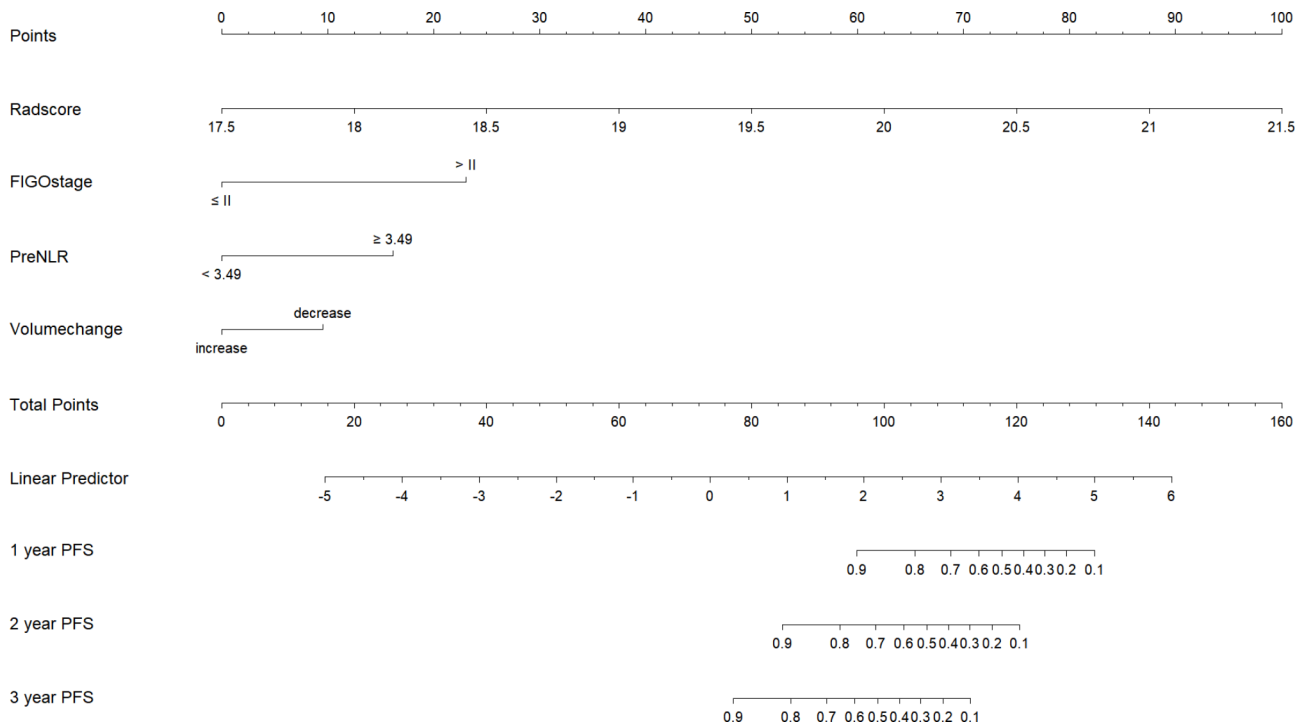


Fig. 6 The nomogram for predicting PFS based on spleen radiomic features and clinical factors

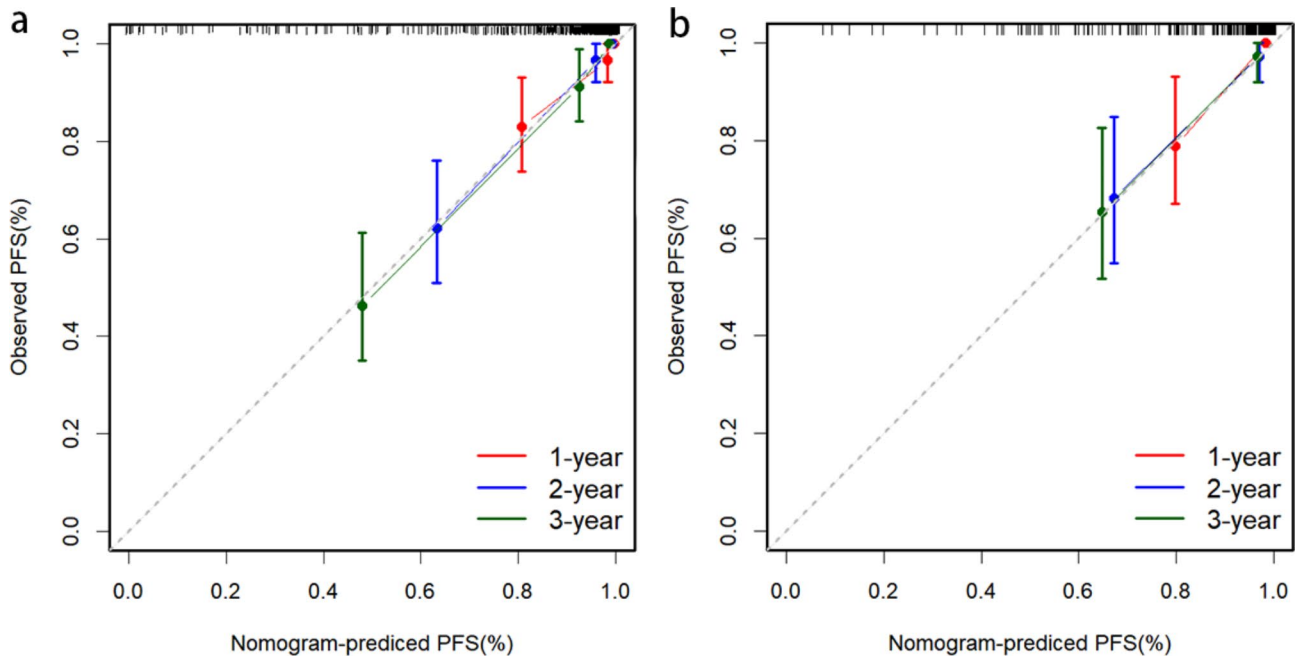


Fig. 7 The calibration curve of the nomogram for predicting 1-, 2- and 3-year PFS in the training (a) and validation groups (b)

based on images of the primary cervical lesion to construct radiomics prediction models, which reflect only the local tumor microenvironment and do not provide insights into systemic immunity. Since cancer is a systemic disease, the status of systemic immunity is closely related to prognosis [13]. Therefore, for a comprehensive

evaluation of systemic immunity before and after treatment, we focused on the spleen and its radiomics, given their strong associations with tumor progression and alterations in systemic immunity.

We found that patients in the high-risk group had higher NLR both before and after radiotherapy compared

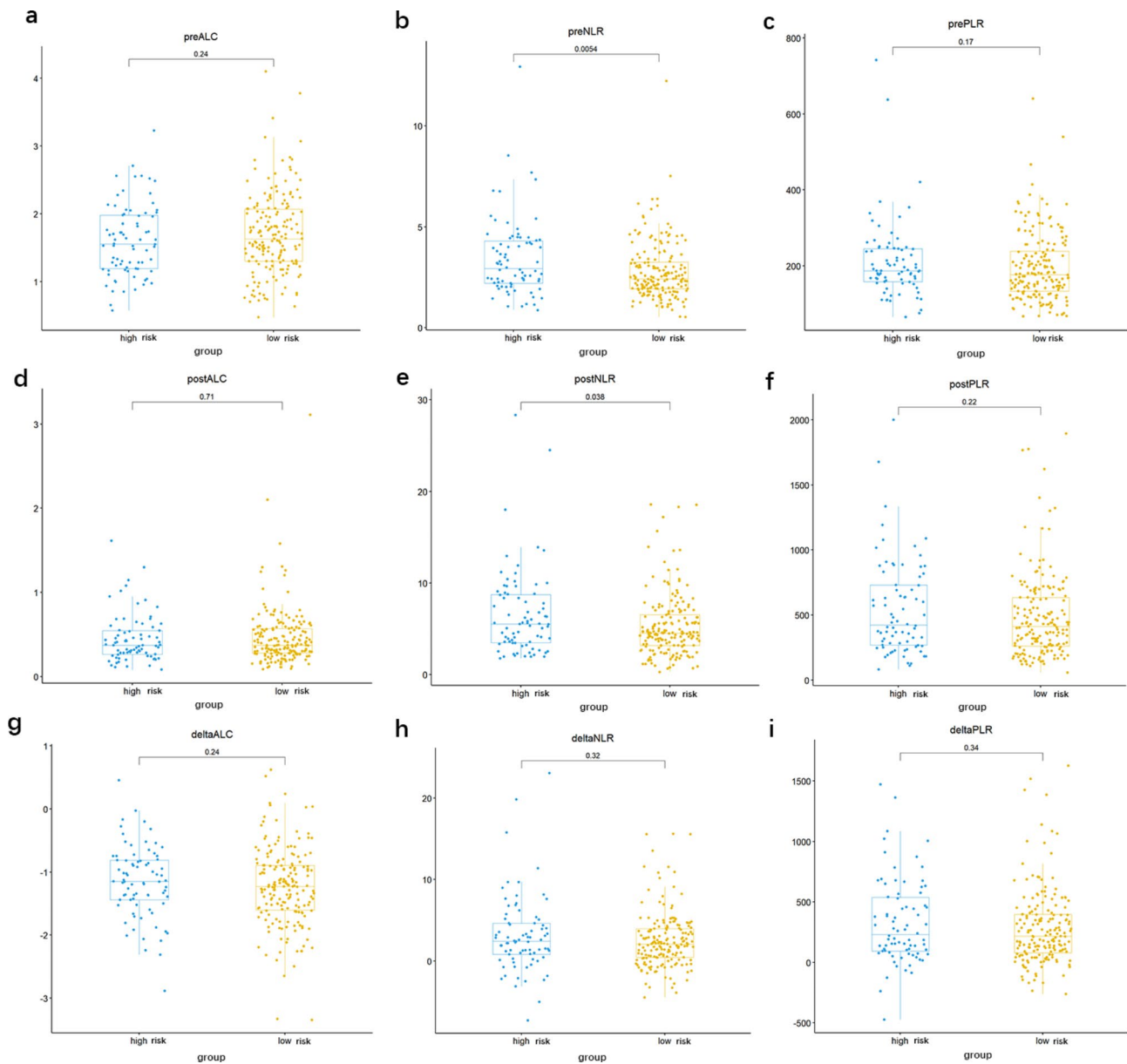


Fig. 8 Box plots comparing immune-related hematological parameters between high-risk and low-risk patient groups: absolute lymphocyte count (ALC), neutrophil-to-lymphocyte ratio (NLR), and platelet-to-lymphocyte ratio (PLR). Specifically, **a**, **b**, and **c** represent comparisons of pre-treatment hematological parameters between the two groups; **d**, **e**, and **f** illustrate post-treatment comparisons; and **g**, **h**, and **i** show comparisons of changes (delta) in these parameters

to those in the low-risk group. This finding supported the existence of a relationship between spleen radiomics and systemic immunity. Increasing research has explored the connection between the spleen and tumor-related systemic inflammation, tumor immune status, and prognosis. Primary tumors induce inflammation, which subsequently modulates immunosuppression through the spleen, thereby impacting patients' immune status [14, 32]. Allen et al. [15] reported an increase in absolute splenocyte counts during tumor growth, and flow cytometry analysis revealed progressive changes in immune status

at the single-cell level in both the tumor and spleen. Similarly, Zeng et al. [33] observed that changes in spleen volume were associated with peripheral immune alterations, including changes in NLR, CD4⁺ T cells, CD8⁺ T cells, and natural killer cells. They specifically highlighted a negative correlation between spleen volume and CD4⁺ T cell counts. The association between the spleen, tumor development, and systemic immunity supports the notion that the spleen can serve as an indicator for detecting systemic immunity in patients after treatment.

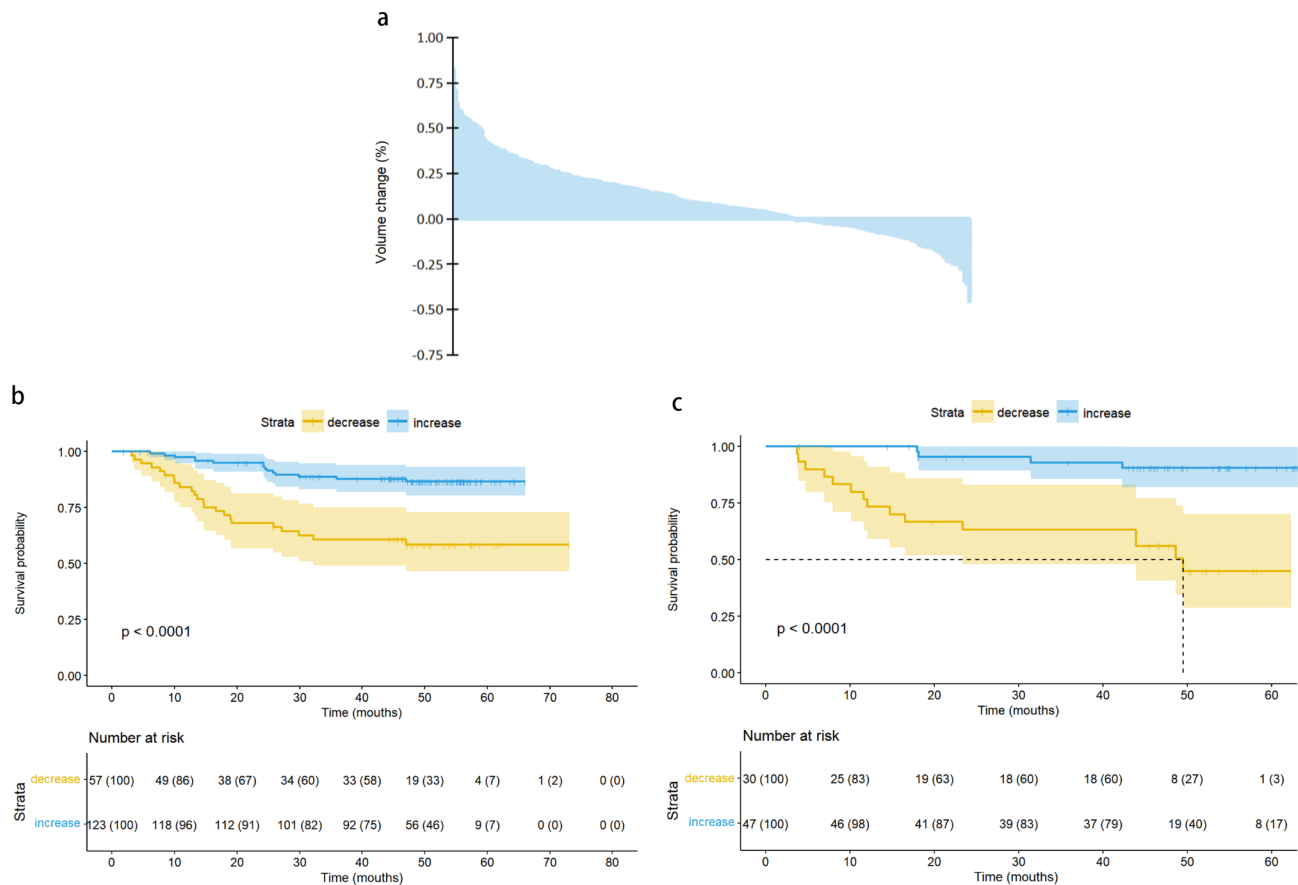


Fig. 9 **a** is the Bar plot for reflecting the spleen volume change for all patients. **b** and **c** are Kaplan-Meier curves for PFS in training group and validation group, with patients stratified according to spleen volume change

Treatment-induced changes in spleen volume can reflect alterations in systemic immunity and serve as a prognostic indicator. In patients with metastatic renal cell carcinoma who underwent immunotherapy, the median spleen volume change was 10% (ranging from -22% to +117%). Increased spleen volume was associated with worse overall survival and PFS [34]. Similarly, in patients with metastatic colorectal cancer who received chemotherapy combined with antiangiogenic therapy, a spleen volume greater than 180 mL was associated with poor PFS [35]. Current research primarily focused on patients with metastatic cancer undergoing immunotherapy, where a high tumor burden leads to extensive disruption of hematopoiesis, as evidenced by the peripheral expansion of immature neutrophils and monocytes [13]. Consequently, an increase in spleen volume in these cases may primarily reflect a state of immune suppression and correlate with poorer prognosis. In contrast, our study involved patients with locally advanced tumors, who generally had a relatively better systemic immune status. Additionally, radiotherapy not only reduces tumor burden but also promotes proliferation and activation through immunogenic cell death, leading to a positive

immunomodulatory effect [8, 9]. Therefore, increased spleen volume after radiotherapy may indicate an activated immune system, correlating with an improved prognosis. Our results demonstrated that in patients with LACC who underwent dCRT, increased spleen volume was associated with improved PFS.

To further investigate the systemic immunity reflected by different changes in spleen volume after radiotherapy, we conducted a comparative analysis of hematological parameters between patients with increased and decreased spleen volume. We found that patients with increased spleen volume exhibited lower NLR and PLR after pelvic radiotherapy. Lower NLR and PLR are associated with better survival and higher immune response rates [36–38]. Therefore, our results indicated that patients with increased spleen volume had a better systemic immune status after radiotherapy compared to those with decreased spleen volume. Further research is needed to understand the reasons behind changes in spleen volume, particularly focusing on alterations in myeloid-derived suppressor cells within the spleen after radiotherapy. Identifying the optimal time to intervene

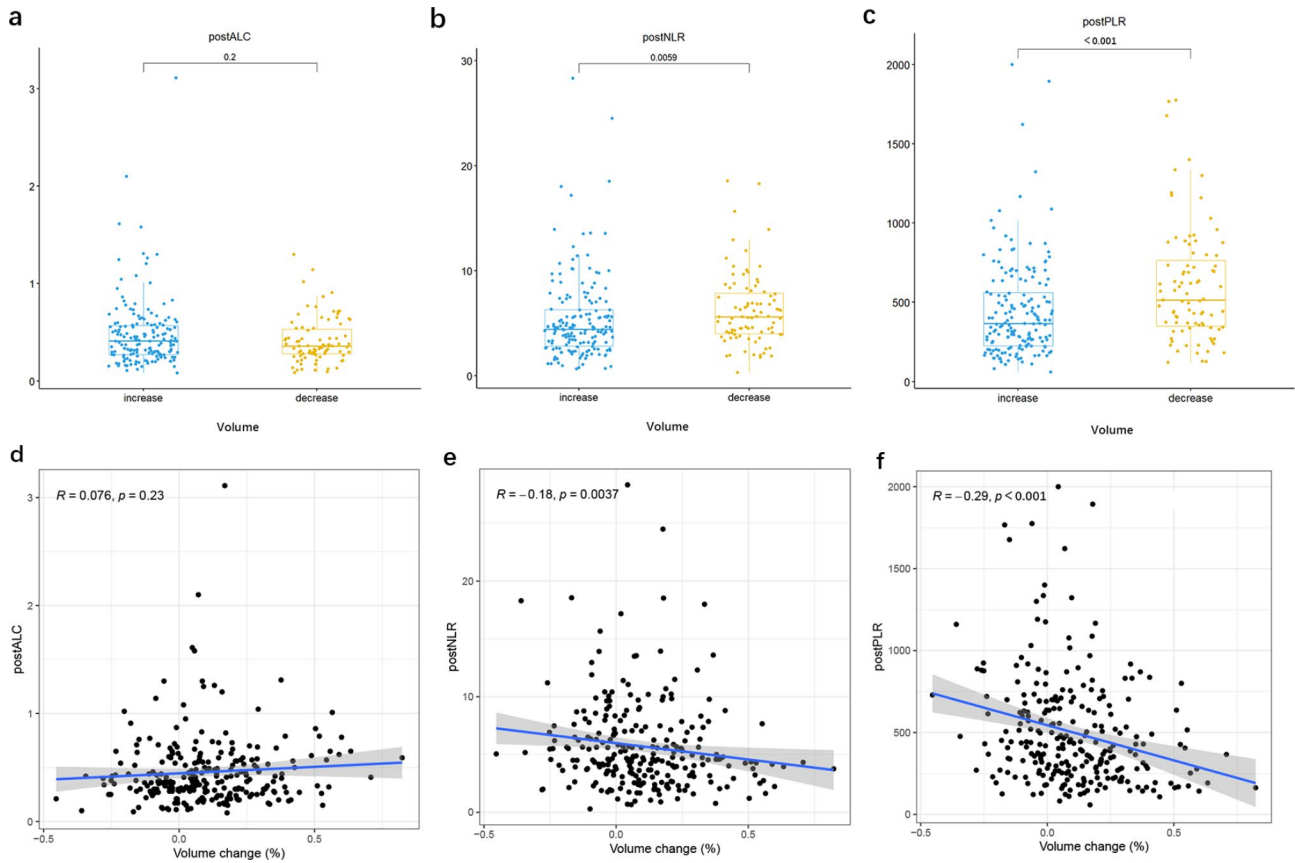


Fig. 10 **a, b** and **c** are comparisons of hematological parameters between the two groups of patients with increased and decreased spleen volume after treatment: absolute lymphocyte count, (ALC)neutrophil-to-lymphocyte ratio (NLR), and platelet-lymphocyte ratio (PLR), respectively. **d, e** and **f** are the correlations between spleen volume change and these parameters after treatment using Spearman correlation analysis

Table 5 Univariate and Multivariate Logistic analysis for distant metastasis

Variable	Cut-off	Univariate analysis		Multivariate analysis	
		OR (95%CI)	P	OR (95%CI)	P
Age, years	≥ 61 vs. < 61	1.29 (0.52 ~ 3.18)	0.578		
FIGO stage	> II vs. ≤ II	4.23 (1.25 ~ 14.30)	0.020	2.53 (0.65 ~ 9.79)	0.180
Tumor size, cm	Continuous	1.34 (1.07 ~ 1.67)	0.012	1.18 (0.91 ~ 1.54)	0.222
Pelvic LN status	N1 vs. N0	1.04 (0.48 ~ 2.24)	0.924		
Spleen volume change	decrease vs. increase	3.08 (1.49 ~ 6.39)	0.002	1.40 (0.58 ~ 3.34)	0.451
BT dose, Gy	≥ 30 vs. < 30	1.00 (0.28 ~ 3.57)	0.998		
EBRT dose, Gy	≥ 50.4 vs. < 50.4	1.02 (0.48 ~ 2.16)	0.963		
pre-ALC, x10 ⁹ cells/L	≥ 1.1 vs. < 1.1	0.38 (0.16 ~ 0.86)	0.021	0.84 (0.23 ~ 3.04)	0.794
post-ALC, x10 ⁹ cells/L	≥ 0.7 vs. < 0.7	1.11 (0.40 ~ 3.09)	0.843		
delta-ALC, x10 ⁹ cells/L	≥ -0.86 vs. < -0.86	2.90 (1.39 ~ 6.05)	0.005	1.64 (0.50 ~ 5.35)	0.416
pre-NLR	≥ 3.49 vs. < 3.49	5.97 (2.81 ~ 12.72)	< 0.001	2.61 (1.04 ~ 6.52)	0.040
post-NLR	≥ 8.09 vs. < 8.09	1.31 (0.55 ~ 3.09)	0.540		
delta-NLR	≥ 15.59 vs. < 15.59	2.15 (0.22 ~ 21.24)	0.513		
pre-PLR	≥ 226.49 vs. < 226.49	3.07 (1.48 ~ 6.35)	0.003	1.50 (0.59 ~ 3.82)	0.398
post-PLR	≥ 787.5 vs. < 787.5	2.93 (1.30 ~ 6.60)	0.009	2.14 (0.79 ~ 5.80)	0.133
delta-PLR	≥ 384.31 vs. < 384.31	1.89 (0.91 ~ 3.93)	0.087		
Radscore	Continuous	7.11 (3.13 ~ 16.14)	< 0.001	4.84 (1.92 ~ 12.24)	< 0.001

Abbreviations: FIGO, Fédération Internationale de Gynécologie et d’Obstétrique; LN, lymph node; BT, brachytherapy; EBRT, external beam radiation therapy; ALC, Absolute lymphocyte counts; NLR, Neutrophil-to-lymphocyte ratio; PLR, Platelet-to-lymphocyte ratio

and prevent the accumulation of these suppressor cells during this process is essential.

Our findings indicated that higher Radscore and pre-NLR were associated with an increased risk of distant metastasis. Additionally, higher Radscore and pre-NLR indicated poorer systemic immunity in these patients. Growing evidence highlights that the interaction between the host immune system and the tumor microenvironment is critical in the progression and metastasis of cervical cancer [39–41]. Notably, significant improvements in PFS were observed in patients with LACC treated with chemoradiotherapy combined with pembrolizumab [42]. Therefore, it is essential to enhance both immune monitoring and immunotherapy to overcome immune suppression, establish local control, and prevent systemic tumor spread. Considering that immune responders after immunotherapy are associated with increased spleen volume and metabolic activity [43], we hypothesize that spleen radiomics features may also undergo change, particularly the weight coefficients of “shape” features. Thus, non-invasive spleen monitoring is crucial in the era of immunotherapy, especially for predicting treatment efficacy and recurrence patterns through changes in specific spleen radiomics features in patients with LACC [3].

This study has several limitations. First, we primarily observed changes in spleen radiomics and volume before and after treatment; further investigation of dynamic changes during treatment is needed. Second, as a single-center retrospective study, our findings need validation through larger, external studies. Future research will involve collaboration with multiple centers to comprehensively validate the prognostic role of spleen radiomics.

Conclusions

Spleen radiomics and volume changes could serve as valuable indicators in assessing systemic immunity and predicting prognosis in patients with LACC who underwent dCRT. Further exploration of the role of the spleen in systemic immune changes following treatment is essential, as it may offer new insights for clinical decision-making.

Abbreviations

LACC	Locally advanced cervical cancer
dCRT	definitive chemoradiotherapy
PFS	Progression-free survival
ALC	Absolute lymphocyte count
NLR	Neutrophil-to-lymphocyte ratio
PLR	Platelet-to-lymphocyte ratio
EBRT	External beam radiation therapy
IMRT	Intensity-modulated radiation therapy
SIB	Simultaneous integrated boost
RECIST	Response Evaluation Criteria in Solid Tumors
PCAS	Picture Archiving and Communication System
ROI	Region of interest
GLCM	Gray level co-occurrence matrix
GLRLM	Gray level run length matrix
GLSZM	Gray level size zone matrix

GLDM	Gray level dependence matrix
NGTDM	Neighborhood gray-tone difference matrix
ICC	Intra-group correlation coefficient
LASSO	Least absolute shrinkage and selection operator
ROC	Receiver operating characteristic
KM	Kaplan–Meier
C-index	Concordance index

Supplementary Information

The online version contains supplementary material available at <https://doi.org/10.1186/s12880-024-01492-1>.

Supplementary Material 1

Supplementary Material 2

Acknowledgements

We would like to sincerely thank the staff in the Department of Radiation Oncology, Shandong Cancer Hospital.

Author contributions

Conceptualization, ML and AL; methodology, YL; software, YL, LG and AL; formal analysis, YL, LG, PX and YL; data curation, LG, YL and YL; writing original draft preparation, YL, LG, and YL; writing review and editing, ML, AL, YL and LG; funding acquisition, ML. YL and LG contributed equally to this study. All authors have read and agreed to the published version of the manuscript. All authors read and approved the final manuscript.

Funding

This work was supported by the National Natural Science Foundation of China [Grant Number 2019QLQN09] and the Key Research and Development Program of Shandong (Major Science & Technology Innovation Project) [Grant Number 2021SFGC0501].

Data availability

The datasets generated and/or analysed during the current study are not publicly available due this study is based on registry data from Shandong Cancer Hospital and Research Institute, which the authors do not own, but are available from the corresponding author on reasonable request.

Declarations

Ethics approval and consent to participate

Our retrospective study abided by the rules of medical ethics, and the Institutional Review Board (IRB) of Shandong Cancer Hospital approved this study. The number for the ethical statement was SDTHEC2024006159. All patients were informed before treatment, agreed to receive concurrent dCRT and signed informed consent forms. We protected patient privacy and excluded patient identification information from our analysis.

Consent for publication

Not applicable.

Competing interests

The authors declare no competing interests.

Author details

¹Department of Radiation Oncology, Shandong Cancer Hospital and Institute, Shandong First Medical University, Shandong Academy of Medical Sciences, Jinan 250117, China

²Department of Gynecologic Radiation Oncology, Shandong Cancer Hospital and Institute, Shandong First Medical University, Shandong Academy of Medical Sciences, Jinan, China

³Department of Radiology, Shandong Cancer Hospital and Institute, Shandong First Medical University, Shandong Academy of Medical Sciences, Jinan, China

⁴School of Clinical Medicine, Shandong Second Medical University, Weifang 261053, China

⁵Department of Radiation Oncology, Cheeloo College of Medicine, Qilu Hospital, Shandong University, Jinan, China

⁶Department of Radiation Oncology, Cheeloo College of Medicine, Shandong Cancer Hospital, Shandong University, Jinan, China

Received: 20 July 2024 / Accepted: 5 November 2024

Published online: 15 November 2024

References

- Bray F, Laversanne M, Sung H et al. Global cancer statistics 2022: GLOBOCAN estimates of incidence and mortality worldwide for 36 cancers in 185 countries[J]. *CA Cancer J Clin*, 2024.
- Ferrari F, Giannini A. Approaches to prevention of gynecological malignancies[J]. *BMC Womens Health*. 2024;24(1):254.
- D'oria O, Bogani G, Cuccu I, et al. Pharmacotherapy for the treatment of recurrent cervical cancer: an update of the literature[J]. *Expert Opin Pharmacother*. 2024;25(1):55–65.
- Schmid MP, Lindegaard JC, Mahantshetty U, et al. Risk factors for local failure following chemoradiation and magnetic resonance image-guided brachytherapy in locally advanced cervical cancer: results from the EMBRACE-I Study[J]. *J Clin Oncol*. 2023;41(10):1933–42.
- Mayadev JS, Ke G, Mahantshetty U, et al. Global challenges of radiotherapy for the treatment of locally advanced cervical cancer[J]. *Int J Gynecol Cancer*. 2022;32(3):436–45.
- Sturza AE, Knoth J. Image-guided brachytherapy in cervical cancer including fractionation[J]. *Int J Gynecol Cancer*. 2022;32(3):273–80.
- Lee J, Lin JB, Chang CL, et al. Optimal prophylactic para-aortic radiotherapy in locally advanced cervical cancer: anatomy-based versus margin-based delineation[J]. *Int J Gynecol Cancer*. 2022;32(5):606–12.
- Fucikova J, Kepp O, Kasikova L, et al. Detection of immunogenic cell death and its relevance for cancer therapy[J]. *Cell Death Dis*. 2020;11(11):1013.
- Galluzzi L, Vitale I, Warren S et al. Consensus guidelines for the definition, detection and interpretation of immunogenic cell death[J]. *J Immunother Cancer*, 2020, 8(1).
- Liang H, Deng L, Chmura S, et al. Radiation-induced equilibrium is a balance between tumor cell proliferation and T cell-mediated killing[J]. *J Immunol*. 2013;190(11):5874–81.
- Romero I, Garrido C, Algarra I, et al. T lymphocytes restrain spontaneous metastases in permanent dormancy[J]. *Cancer Res*. 2014;74(7):1958–68.
- Spitzer MH, Carmi Y, Reticker-Flynn NE, et al. Systemic immunity is required for effective Cancer Immunotherapy[J]. *Cell*. 2017;168(3):487–e50215.
- Hiam-Galvez KJ, Allen BM, Spitzer MH. Systemic immunity in cancer[J]. *Nat Rev Cancer*. 2021;21(6):345–59.
- Lewis SM, Williams A, Eisenbarth SC. Structure and function of the immune system in the spleen[J]. *Sci Immunol*, 2019, 4(33).
- Allen BM, Hiam KJ, Burnett CE, et al. Systemic dysfunction and plasticity of the immune macroenvironment in cancer models[J]. *Nat Med*. 2020;26(7):1125–34.
- Kim SY, Moon CM, Yoon HJ, et al. Diffuse splenic FDG uptake is predictive of clinical outcomes in patients with rectal cancer[J]. *Sci Rep*. 2019;9(1):1313.
- Seban RD, Rouzier R, Latouche A, et al. Total metabolic tumor volume and spleen metabolism on baseline [18F]-FDG PET/CT as independent prognostic biomarkers of recurrence in resected breast cancer[J]. *Eur J Nucl Med Mol Imaging*. 2021;48(11):3560–70.
- De Jaeghere EA, Laloo F, Lippens L, et al. Splenic (18)F-FDG uptake on baseline PET/CT is associated with oncological outcomes and tumor immune state in uterine cervical cancer[J]. *Gynecol Oncol*. 2020;159(2):335–43.
- Yoon HJ, Kim BS, Moon CM, et al. Prognostic value of diffuse splenic FDG uptake on PET/CT in patients with gastric cancer[J]. *PLoS ONE*. 2018;13(4):e0196110.
- Vandendorpe B, Durot C, Lebellec L, et al. Prognostic value of the texture analysis parameters of the initial computed tomographic scan for response to neoadjuvant chemoradiation therapy in patients with locally advanced rectal cancer[J]. *Radiother Oncol*. 2019;135:153–60.
- Liu Z, Wang S, Dong D, et al. The applications of Radiomics in Precision diagnosis and treatment of Oncology: opportunities and Challenges[J]. *Theranostics*. 2019;9(5):1303–22.
- Wang X, Sun J, Zhang W, et al. Use of radiomics to extract splenic features to predict prognosis of patients with gastric cancer[J]. *Eur J Surg Oncol*. 2020;46(10 Pt A):1932–40.
- Chen C, Liu J, Gu Z, et al. Integration of Multimodal Computed Tomography Radiomic Features of Primary Tumors and the spleen to predict early recurrence in patients with postoperative adjuvant Transarterial Chemoembolization[J]. *J Hepatocell Carcinoma*. 2023;10:1295–308.
- Zhu M, Feng M, He F, et al. Pretreatment neutrophil-lymphocyte and platelet-lymphocyte ratio predict clinical outcome and prognosis for cervical Cancer[J]. *Clin Chim Acta*. 2018;483:296–302.
- Onal C, Guler OC, Yildirim BA. Prognostic use of pretreatment hematologic parameters in patients receiving definitive chemoradiotherapy for cervical Cancer[J]. *Int J Gynecol Cancer*. 2016;26(6):1169–75.
- Pujade-Lauraine E, Tan DSP, Leary A, et al. Comparison of global treatment guidelines for locally advanced cervical cancer to optimize best care practices: a systematic and scoping review[J]. *Gynecol Oncol*. 2022;167(2):360–72.
- Abu-Rustum NR, Yashar CM, Arend R, et al. NCCN Guidelines® insights: Cervical Cancer, Version 1.2024[J]. *J Natl Compr Canc Netw*. 2023;21(12):1224–33.
- Watanabe H, Okada M, Kaji Y, et al. [New response evaluation criteria in solid tumours-revised RECIST guideline (version 1.1)] [J]. *Gan Kagaku Ryoho*. 2009;36(13):2495–501.
- Chen X, Liu W, Thai TC, et al. Developing a new radiomics-based CT image marker to detect lymph node metastasis among cervical cancer patients[J]. *Comput Methods Programs Biomed*. 2020;197:105759.
- Wu RR, Zhou YM, Xie XY, et al. Delta radiomics analysis for prediction of intermediary- and high-risk factors for patients with locally advanced cervical cancer receiving neoadjuvant therapy[J]. *Sci Rep*. 2023;13(1):19409.
- Sun C, Tian X, Liu Z, et al. Radiomic analysis for pretreatment prediction of response to neoadjuvant chemotherapy in locally advanced cervical cancer: a multicentre study[J]. *EBioMedicine*. 2019;46:160–9.
- Han Y, Liu Q, Hou J, et al. Tumor-Induced Generation of Splenic Erythroblast-like ter-cells promotes Tumor Progression[J]. *Cell*. 2021;184(5):1392.
- Zeng Z, Liu Z, Li J, et al. Baseline splenic volume as a biomarker for clinical outcome and circulating lymphocyte count in gastric cancer[J]. *Front Oncol*. 2022;12:1065716.
- Aslan V, Karabörk Kılıç AC, Özet A, et al. The role of spleen volume change in predicting immunotherapy response in metastatic renal cell carcinoma[J]. *BMC Cancer*. 2023;23(1):1045.
- Niogret J, Limagne E, Thibaudin M et al. Baseline splenic volume as a Prognostic Biomarker of FOLFIRI Efficacy and a surrogate marker of MDSC Accumulation in metastatic colorectal Carcinoma[J]. *Cancers (Basel)*, 2020, 12(6).
- Trinh H, Dzul SP, Hyder J, et al. Prognostic value of changes in neutrophil-to-lymphocyte ratio (NLR), platelet-to-lymphocyte ratio (PLR) and lymphocyte-to-monocyte ratio (LMR) for patients with cervical cancer undergoing definitive chemoradiotherapy (dCRT)[J]. *Clin Chim Acta*. 2020;510:711–6.
- Zhang N, Jiang J, Tang S, et al. Predictive value of neutrophil-lymphocyte ratio and platelet-lymphocyte ratio in non-small cell lung cancer patients treated with immune checkpoint inhibitors: a meta-analysis[J]. *Int Immunopharmacol*. 2020;85:106677.
- Diem S, Schmid S, Krapf M, et al. Neutrophil-to-lymphocyte ratio (NLR) and platelet-to-lymphocyte ratio (PLR) as prognostic markers in patients with non-small cell lung cancer (NSCLC) treated with nivolumab[J]. *Lung Cancer*. 2017;111:176–81.
- Sherer MV, Kotha NV, Williamson C, et al. Advances in immunotherapy for cervical cancer: recent developments and future directions[J]. *Int J Gynecol Cancer*. 2022;32(3):281–7.
- Colombo N, Dubot C, Lorusso D, et al. Pembrolizumab for Persistent, recurrent, or metastatic cervical Cancer[J]. *N Engl J Med*. 2021;385(20):1856–67.
- Duska LR, Scalici JM, Temkin SM, et al. Results of an early safety analysis of a study of the combination of pembrolizumab and pelvic chemoradiation in locally advanced cervical cancer[J]. *Cancer*. 2020;126(22):4948–56.
- Lorusso D, Xiang Y, Hasegawa K, et al. Pembrolizumab or placebo with chemoradiotherapy followed by pembrolizumab or placebo for newly diagnosed, high-risk, locally advanced cervical cancer (ENGOT-cx11/GOG-3047/KEYNOTE-A18): a randomised, double-blind, phase 3 clinical trial[J]. *Lancet*. 2024;403(10434):1341–50.
- Seith F, Forschner A, Weide B et al. Is there a link between very early changes of primary and secondary lymphoid organs in (18)F-FDG-PET/MRI and treatment response to checkpoint inhibitor therapy?[J]. *J Immunother Cancer*, 2020, 8(2).

Publisher's note

Springer Nature remains neutral with regard to jurisdictional claims in published maps and institutional affiliations.